

The Role of Declining Snow Cover in the Desiccation of the Great Salt Lake, Utah, using MODIS Data

Dorothy K. Hall^{1,2}, Donal S. O’Leary III³, Nicolo E. DiGirolamo^{4,2}, Woodruff Miller⁵ and Do Hyuk Kang^{1,2}

¹Earth System Science Interdisciplinary Center, University of Maryland, College Park, MD 20740 dkhall1@umd.edu, dk.kang@nasa.gov

²NASA / Goddard Space Flight Center, Greenbelt, MD 20771

³Department of Geographical Sciences, University of Maryland, College Park, MD 20742 donalsoleary3@gmail.com

⁴SSAI, Lanham, MD 20706 nicolo.e.digirolamo@nasa.gov

⁵Civil and Environmental Engineering, Brigham Young University, Provo, UT 84602 wood_miller@byu.edu

Abstract

The Great Salt Lake (GSL) in Utah has been shrinking since the middle of the 19th Century, leading to decreased area and volume, and increased salinity. We use satellite data products from the Terra and Aqua MODerate-resolution Imaging Spectroradiometer (MODIS) and the Landsat-7 and -8 satellites, along with meteorological and streamflow data, and modeled data products to study the relationship between changing snow-cover conditions and the decline of the GSL since 2000 in the context of the historical record of lake levels. The GSL basin includes much of the snow-dominated Wasatch and Uinta mountain ranges to the east of the lake. Snowmelt feeds the Bear, Jordan, and Weber rivers which are the three main rivers that flow into the lake. Snowmelt-timing maps, derived from a new MODIS standard snow-cover product, MOD10A1F, show that snow melted ~9.5 days earlier in the GSL basin during the study period, extending from 2000 – 2018. Air temperatures derived from 26 meteorological stations and surface temperatures measured by the Aqua MODIS land-surface temperature (LST) products, MYD21A1D and MYD21A1N, show trends of increasing temperature of ~0.94°C ($\alpha=0.05$), and ~2.18°C, respectively, with most of the LST trends in the GSL basin being statistically significant ($\alpha=0.05$). Increasing air temperatures in the basin have led to less precipitation falling as snow, lower snow depth (by ~34.5 mm ($\alpha=0.01$)) and snow-water equivalent (0.02 mm ($\alpha=0.01$)), and earlier snowmelt. Also during the study period, Global Land surface Evaporation Amsterdam Model data show evaporation increasing by ~3.2 mm/yr, with trends in much of the basin being statistically significant ($\alpha=0.05$). Trends calculated from the various products are generally in agreement indicating higher temperatures, greater evaporation, less snowfall and snow-on-the ground, and earlier snowmelt. Earlier snowmelt contributes to increasing evaporative loss from water flowing toward the lake. Furthermore, a lower mountain snowpack and less precipitation falling as snow (versus rain) is associated with lower stream discharge *even if overall precipitation stays the same*. The surface-water temperature of the GSL also increased over the study period by ~0.69°C, according to the MODIS LST data products, and the surface-water elevation of the lake dropped by ~1.7 m between 2000 and 2018 based on United States Geological Survey measurements, and the areal extent of the lake decreased by ~901 km² as measured using Landsat imagery. Desiccation of the lake is associated with deleterious effects on wildlife, recreational activities, and some local industries. And, importantly, an expanding

lake bed can also fuel dust storms that promote dangerous air quality along the Wasatch Front. This work elucidates the key role that satellite remote sensing can play in documenting earlier snowmelt and other changes in the GSL basin that influence the ongoing decline of the Great Salt Lake.

1. Introduction

Globally, saline lakes have been shrinking primarily due to increasing water demand by humans (Wurstbaugh et al., 2017). The Great Salt Lake (GSL) in Utah is the largest salt-water lake in the Western Hemisphere, covering an area of $\sim 4400 \text{ km}^2$ at the historic average (1847-1986) (Utah Water Science Center, 2020). However, in recent years the GSL has experienced some of the lowest surface-water elevations in the historical record (Frankson and Kunkel, 2016). The GSL is a terminal lake, meaning that it has no outlets, losing water almost exclusively through evaporation. Fluctuation in streamflow is the dominant factor in lake-level fluctuations (Mohammed and Tarboton, 2012). Since the middle of the 19th Century, the amount of water flowing into the GSL has been reduced by ~ 39 percent because of upstream diversions causing the volume of the lake to decrease by ~ 48 percent, and the area to decrease by ~ 50 percent (Wurstbaugh et al., 2016 & 2017). Every year, 3.3 trillion liters of water are diverted from the streams feeding the GSL (Derouin, 2017), contributing to a surface-water elevation drop of ~ 3.6 m. This precipitous decline is caused primarily by upstream diversions of water for agricultural and other uses beginning with the arrival of the pioneers in 1847, but has been exacerbated by the warming climate (Wurstbaugh et al., 2017; Wang et al., 2018).

The Bear, Jordan, and Weber rivers are heavily utilized for agricultural and other purposes in this arid region, thus there are many diversions and reservoirs upstream of the lake. For example, in 1911-12 the Bear River was diverted into Bear Lake so that Bear Lake could be used as a reservoir (Utah Water Science Center, 2020). For the Weber River, there are more than 200 irrigation diversions (Utah's Watershed Restoration Initiative, 2019). Furthermore, dams have been built to facilitate irrigation, such as the Turner Dam and the Joint Dam on the Jordan River. To further complicate matters, 71 percent of the treated wastewater from cities and towns on the Wasatch Front is discharged into or near the lake (Maffly, 2015; Penrod, 2019).

The streams in the GSL basin that flow into the GSL originate in the snow-covered Wasatch and Uinta mountains to the east of the lake. Interannual differences in snow depth in the mountains represent the primary influence on natural fluctuation of water level in the GSL. The lake depth is greatest in springtime because of inflow from melting snow from the mountains. In wet years when there is a large snowpack, the lake level increases. In dry years, the lake level falls. Nevertheless, because there are reservoirs, diversions of upstream waters and wastewater discharge into the lake, it is problematic to relate changing snow conditions in the GSL basin to trends in stream discharge using stream-gauge data.

The Great Salt Lake is a vital stopover for millions of migratory birds and waterfowl that must feed, nest and rest during their journeys. However as the volume of water in the lake decreases, the salinity increases and there are fewer wetlands, thus jeopardizing primary food sources for

migrating birds such as brine shrimp and brine flies (Audubon, 2020). Brine shrimp are also harvested by humans as food for fish, and exported worldwide.

As the lake level falls, the areal extent of the lake shrinks; the lake is very shallow with a maximum depth of ~10 m at the historical average surface elevation of 1280 m (Utah Geological Survey, 2020) and therefore small changes in lake volume can cause significant changes in the extent of the lake (Baskin, 2005). An expanding dry lake bed is a major source of dust pollution (Reynolds et al., 2014) and can accelerate snowmelt in the nearby mountains when dust is blown onto the snow, reducing the albedo of the snow surface and allowing greater absorption of solar radiation (Skiles et al., 2018).

An ongoing drought in the western United States has been exacerbated by warmer temperatures (Christensen and Lettenmaier, 2006; McCabe and Wolock, 2007; Udall and Overpeck, 2017; Williams et al., 2020) causing reduced river flows due to greater evaporative losses and earlier snowmelt (Milly and Dunne, 2020). In the state of Utah, there is a trend of increasing temperature, including a dramatic increase in nighttime temperature since 1990 (Frankson and Kunkel, 2016). Global climate models predict increasing temperatures through the 21st Century with an increase in the fraction of precipitation falling as rain versus snow, thus decreasing snowpack water storage (Frankson and Kunkel, 2016). The intensity of droughts is also projected to increase (McKenzie and Littell, 2017).

Recent advances in remote-sensing science have allowed for additional insights into the desiccation of the GSL using Moderate-resolution Imaging Spectroradiometer (MODIS) and other satellite data products. The Terra satellite carrying a MODIS instrument was launched in December of 1999, and a second MODIS instrument was launched on the Aqua satellite in May of 2002. MODIS has 36 bands with spatial resolution ranging from 250 m to 1-km resolution. MODIS data from each satellite are obtained daily or every-other-day everywhere on the Earth, cloud-cover permitting. The MODIS record now spans two decades, providing a decade-scale time series. The Landsat record began in 1972, and continues today with the Landsat-8 Operational Land Imager (OLI) which provides higher spatial resolution (30 m) relative to the MODIS and nearly five decades of data, but less-frequent coverage than is obtained by MODIS.

In this paper, we explore the role of decreasing snow cover in the GSL basin in the ongoing desiccation of the GSL, using primarily new MODIS standard products and taking advantage of the nearly 20-year record. The new daily MODIS cloud-gap filled snow-cover and snowmelt-timing products, the MODIS land-surface temperature (LST), and white-sky albedo (WSA) products, along with modeled data of snow-water equivalent and evaporation, stream-gauge data and meteorological-station data are used both independently and in concert to improve our understanding of the factors responsible for the decline of the GSL.

2. Study Area

2.1 The Great Salt Lake basin

The Great Salt Lake basin is ~89,000 km² in area, including the West Desert basin to the west of the lake (Great Salt Lake Information System, 2020). Streamflow contributes ~66 percent of the

inflow to the GSL, direct precipitation onto the lake contributes ~31 percent and ground water contributes ~3 percent (Arnow and Stephens, 1990; USGS, 2007). The vast majority of surface flow to the GSL basin is from the Bear, Jordan and Weber rivers for which the headwaters are located in the mountains to the east of the lake (Figure 1). Contributing the most streamflow is the Bear (~58 percent), followed by the Jordan (~22 percent) and then the Weber (~15 percent) rivers (Wurtsbaugh et al., 2017). The remaining ~5 percent of surface-water inflow comes from ten tributaries on the east and south shores of the lake (Arnow and Stephens, 1990). We delineated a 35,251 km² region of interest (ROI) (Figure 1) corresponding to the Bear, Jordan and Weber river basins. Herein, we call this ROI the ‘effective area of the GSL basin,’ or simply the GSL basin.

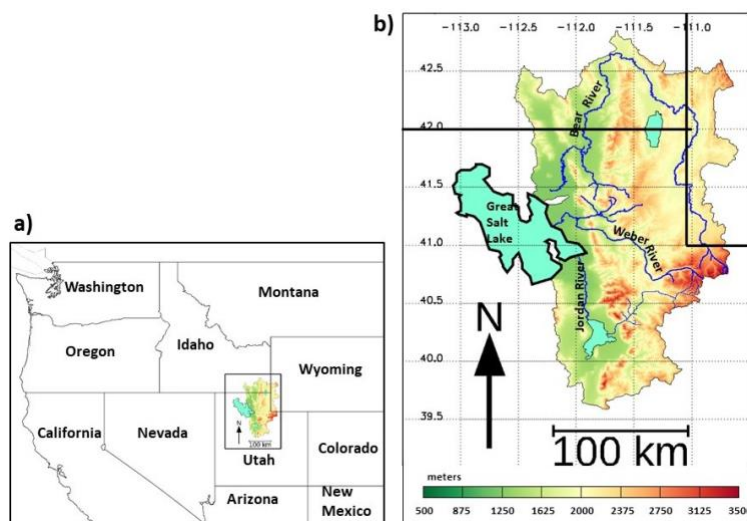


Fig. 1a & 1b. a) Location of the Great Salt Lake (GSL) basin in the western United States. b) The GSL basin is shown along with a Digital-Elevation Model (DEM) developed from the USGS GTOPO30 digital-elevation model (USGS GTOPO30 DEM, 2019), with the different colors depicting different elevations in the basin. The Great Salt Lake, Bear Lake (northeast of the GSL) and Utah Lake (south of the GSL) are shown in aquamarine. State boundaries of Idaho, Wyoming, and Utah are delineated with heavy black lines. The Bear, Jordan and Weber rivers are also shown. The river-basin boundaries were derived from shape files from the USGS National Map (2019).

The north-south trending Wasatch Mountain Range covers an area of approximately 21,000 km², and extends north into Idaho (Figures 1 & 2). Mount Nebo (3637 m) is the highest peak in the Wasatch Range. The Uinta Mountains trend in an east-west direction, extending into Wyoming. Kings Peak (4123 m) in the Uinta Mountains is the highest peak in Utah (Figure 2).



Fig. 2. Image of the Great Salt Lake (GSL) from the MODIS on the Terra satellite acquired on 29 July 2015 during drought conditions, showing color differences between the north (Gunnison Bay) and south (Gilbert Bay) arms of the lake. The GSL basin is outlined in yellow. Utah Lake (light green) is visible southeast of the GSL, and Bear Lake (deep blue) is visible in the northern part of the basin spanning the border between Utah and Idaho. Credit: NASA Worldview (2020).

2.2 Great Salt Lake

A Union Pacific Railroad causeway divides the GSL into north (Gunnison Bay) and south (Gilbert Bay) arms (Figure 2) between which there is very little mixing of water. Streamflow discharges primarily into the south arm causing the water-surface elevation to be ~0.15 - 0.61 m higher and the salinity to be lower than that of the north arm. The salinity of the GSL varies with lake level, averaging ~317 g/L in the north arm and ~142 g/L in the south arm since 1966 (White et al., 2014). By comparison, the average salinity of the world ocean is about 35 g/L. The south arm is generally suited to hosting a large population of brine shrimp and some other hardy creatures such as brine flies. The hypersaline Gunnison Bay contains large populations of salt-tolerant bacteria and an alga with a red pigment, causing the reddish color seen in the MODIS image (Figure 2).

2.3 Precipitation in the Great Salt Lake basin

Though winter precipitation in Utah has increased over the last 50 years (Bedford and Douglass, 2008; Gillies et al., 2012), the proportion of winter precipitation falling as snow has decreased by 9 percent, and snow depths and snow extent across the state of Utah have also declined (Gillies et al., 2012), consistent with declines in average April 1 snow-water equivalent (SWE) across the western U.S. (Mote et al., 2018). About 30-40 percent of the precipitation that falls in the Wasatch Mountains runs off, 40-60 percent is lost to evapotranspiration and sublimation, and the remaining goes to regional groundwater recharge (Manning, 2002).

Most of the precipitation in northern Utah occurs during the winter in the form of snow (Carson, 2007). Storms that deposit snow in the Wasatch and Uinta mountains typically originate in the Pacific Ocean and cross the Sierras or Cascades on their journey eastward before reaching the

mountains, losing moisture as they travel inland. The "Greatest Snow on Earth" reputation of the Wasatch Mountain snow is largely due to the frequency of snowstorms and the characteristic that the many storms tend to deposit snow with increasingly lower SWE as the storm progresses (Steenburgh and Alcott, 2008). This allows for a solid base and a deep layer of dry powdery snow on top which is highly sought-after by skiers.

2.3.1 Precipitation and lake level variations due to the Quasi-Decadal Oscillation

The GSL lake level is sensitive to fluctuations in long-term evaporation and precipitation due to its bathymetry (large surface area and shallow depth) (Lall and Mann, 1995). In addition to annual variations primarily caused by snow deposition in the mountains, lake-level fluctuations are also influenced by climate-forcing mechanisms that are oscillatory. Mann et al. (1995) identified a ~12-year cycle in fluctuations of the GSL lake levels caused by a shifting of storm tracks that influence winter precipitation, explaining ~18 percent of the interannual and longer-term variance in the record of monthly lake-levels.

The impacts of the tropical and North Pacific variability are significant in the western U.S. climate, though less-pronounced in the Great Basin in which the GSL is located (Wang et al., 2010). However the GSL lake levels respond to the transition part of the Pacific Quasi-Decadal Oscillation (QDO). The Pacific QDO has distinct phases of sea-surface temperature and atmospheric circulation patterns including the transition phases in-between the extreme warm and cold (Wang et al. 2010; DeRose et al., 2014). GSL lake levels consistently lag the precipitation, taking ~6 years to respond (Wang et al., 2012). There is a large and important body of literature on the topic of periodic GSL lake-level fluctuations that addresses wet-drought cycles and climate change in the Great Basin, but is beyond the scope of this paper.

2.3.2 Lake-effect snow

When an air mass from the Pacific Ocean travels inland, and over the GSL, lake-effect or lake-enhanced (LE) precipitation may occur when a strong, cold, northwesterly wind blows across the lake causing enhanced evaporation when the cold, dry air mass travels over the relatively-warm lake surface (Steenburgh et al., 2000; Alcott and Steenburgh, 2013). As the air mass continues to travel east, the mountains cause orographic lifting and precipitation falls as the air parcel rises. Precipitation from LE snow occurs over northern Utah several times a year, and is a relatively minor contribution to the total precipitation in the GSL basin (Steenburgh et al., 2000), but when it occurs, it can contribute a substantial amount of snow.

Yaeger et al. (2013) estimated the contribution of precipitation from LE events between 1998 and 2009 during the cool seasons (defined as 16 September – 15 May). They found that the fraction of cool-season SWE from LE snow in the GSL basin is small and localized, with, for example, a maximum of 8.4 percent in the Oquirrh Mountains located to the south of the GSL, though there is great variability in SWE between cool seasons. The high salinity of the GSL reduces the saturation vapor pressure and latent heat flux, thus reducing the amount of moisture from the lake that is available to be added to the air above the lake (Steenburgh et al., 2000; Alcott et al., 2012). While important to the Utah ski industry, LE snowfall in the GSL basin is not a major contributor to the total snow volume, except locally in some years.

3. Data and Methods

To investigate the effect of snow-cover changes in the GSL basin on the desiccation of the lake, we used satellite data products along with meteorological, streamflow and modeled data. National Aeronautics and Space Administration (NASA) Terra MODIS data products were used to study snow-cover changes in the GSL basin during the “MODIS era,” which may be defined as the years 2000 – present. Aqua MODIS data products, available beginning in 2002, were used to measure surface temperature in the GSL basin and in the GSL, and to delineate the changing areal extent of the GSL. Landsat-7 Enhanced Thematic Mapper Plus (ETM+) and Landsat-8 OLI imagery was used to delineate the minimum areal extent of the GSL from 2000 – 2019.

The boundaries of the Bear, Jordan and Weber river basins were derived from shape files from the USGS National Map (2019). The digital-elevation model (DEM) from the USGS GTOPO30 digital-elevation model (USGS GTOPO30 DEM, 2019) was also used.

3.1 Snowmelt-timing maps

We use the MODIS Terra cloud-gap filled (CGF) normalized-difference snow index (NDSI) daily snow-cover product, MOD10A1F, from MODIS Collection 6.1 to provide a snow map of the surface each day. A clear view is achieved by looking back in time to the last cloud-free observation of the surface on a per-pixel basis (Hall et al., 2010 & 2019 and Riggs et al., 2018). The MOD10A1F product was developed and produced at Goddard Space Flight Center (Riggs et al., 2017) and will be distributed by the National Snow and Ice Data Center (NSIDC) beginning in the fall of 2020. MOD10A1F prototype products were used to develop snowmelt-timing maps using the snowmelt-timing algorithm of O’Leary et al. (2017, 2018 & 2020) to calculate the timing of snowmelt in the GSL basin for each water year (WY) from 1 October 2000 through 30 September 2018. Snowmelt-timing maps identify the day of the year that each pixel transitions from snow covered to ‘not snow covered’ during the melt season. To eliminate late-season ephemeral snow, after 31 March each year, the algorithm ignores new snow after 48 snow-free days. A sample snowmelt-timing map for the GSL Basin for the 2018 WY is provided in Figure 3. The MODIS-based snowmelt-timing map product is available through the Oak Ridge National Labs Distributed Active Archive Center (O’Leary et al., 2017).

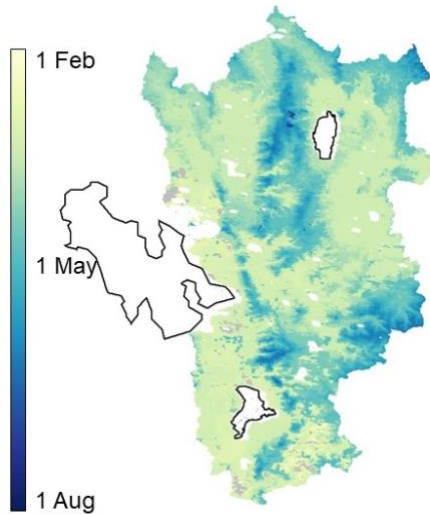


Fig. 3. Snowmelt-timing map of the effective area of the Great Salt Lake basin for the water year 2018 developed using a modification of the algorithm of O’Leary et al. (2017). Bear Lake, Great Salt Lake and Utah Lake are outlined in black. There are a few pixels shown in grey representing the days when melt occurred prior to 1 February 2018.

3.2 Meteorological data

Meteorological data from stations located in the GSL basin were obtained from the NOAA National Climatic Data Center daily summaries maps (NOAA, 2020) and the United States Department of Agriculture SNOTEL stations (SNOTEL, 2020). Figure 4 shows the locations of the 26 stations used in this work. Each station reported for 270 or more days per year for at least 17 years, from 2000 – 2018. Trends in T_{min}, T_{max} and T_{mean} in °C as well as trends in snowfall and snow depth were calculated. All of the stations are below 2000 m except for eight. The station names along with coordinates and elevation are provided in Appendix 1.

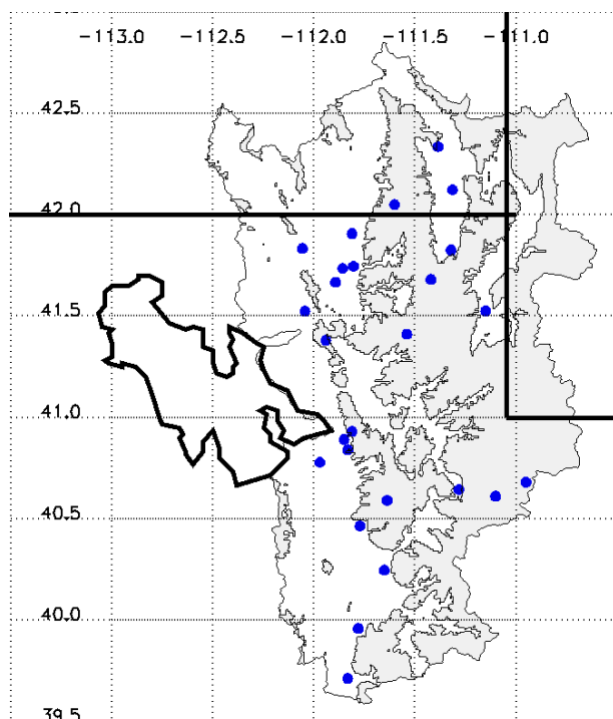


Fig. 4. Meteorological stations used in this work. Blue dots show the locations of 26 stations reporting continuously or nearly continuously from 2000-2018. Thin lines show the boundary of the effective area of the Great Salt Lake basin; shading shows parts of the watershed that are ≥ 2000 m in elevation. The perimeter of the GSL and state boundaries of Utah, Idaho, and Wyoming are shown in thick black lines.

3.3 Stream discharge data

Monthly streamflow data within the GSL basin were analyzed from seven USGS stream gauges along the Bear River, four stations along the Weber River and one station along the Jordan River (USGS, 2020). From the monthly data, we calculated and plotted annual-average discharge data beginning with the first full year following the beginning of the station record, and calculated trends in discharge in m^3/yr . The names, elevations, coordinates and periods of record of the 12 stream gauges that were used in this work are provided in Appendix 2.

3.4 Snow-water equivalent

There is currently no reliable way from space to measure SWE in mountainous areas, however estimates of SWE are provided through modeling. Beginning in 2003, NOAA's National Weather Service (NWS) National Operational Hydrologic Remote Sensing Center (NOHRSC) SNOW Data Assimilation System (SNODAS), included procedures to assimilate satellite-derived, airborne, and ground-based observations of snow-covered area and SWE, to provide estimates of SWE and other parameters in support of hydrologic modeling and analysis (Carroll et al., 2001; NOHRSC, 2004; SNODAS, 2020). Daily SWE from SNODAS was analyzed for the period from WY 2003 – 2018 for the GSL basin.

3.5 Land-surface temperature

Aqua MODIS LST standard data products were used to measure the surface temperature in the GSL basin, and within the lake itself. Terra MODIS LST V006 data products are only available

from 2000 – 2005 (Hulley and Hook, 2017), and were not used in this work because of the relatively-short period of record. The 1-km resolution LST products from the Aqua satellite, MYD21A1D (daytime) and MYD21A1N (nighttime) V006 (Hulley, 2017), extend from 4 July 2002 through the present, providing LST on a per-pixel basis. For the LST trend calculations, we started with the first full year of the Aqua LST dataset which is 2003. The LSTs for the entire basin (excluding the rejected pixels and cloudy pixels) were averaged each day to create a daily-mean LST for the basin.

There were issues with some of the nighttime data from MYD21A1N in the GSL basin and as a result data from many of the pixels had to be rejected. If a pixel had 90 or more consecutive days of ‘no LST’ retrieval, or if a pixel had 16 or more periods of 30+ days of ‘no LST retrieval,’ those pixels were rejected. As a result, an area in the western part of the GSL basin is not used in this work and is therefore ‘greyed-out’ in the resulting LST trend maps and not used in the trend calculations.

3.6 Evaporation

The Global Land surface Evaporation Amsterdam Model (GLEAM) is a dataset consisting of a set of algorithms that uses satellite-derived products to estimate daily evaporation globally at 0.25° spatial resolution (Miralles et al., 2011; Martens et al., 2017). The dataset is based on reanalysis radiation and air temperature, a combination of gauge-based, reanalysis and satellite-based precipitation, and satellite-based vegetation optical depth (GLEAM, 2019). GLEAM provides estimates of the components of terrestrial evaporation based on satellite observations of transpiration, interception loss, bare-soil evaporation, snow sublimation and open-water evaporation. A Priestley-Taylor equation (Priestly and Taylor, 1972) is used to calculate potential evaporation based on observations of surface net radiation and near-surface air temperature. Potential evaporation estimates are then converted into actual evaporation. For this work the GLEAM V3.3a dataset from 2000 – 2018 (GLEAM, 2019) was used for the GSL basin, excluding the GSL itself.

Various approaches have been used to estimate evaporation from the GSL based on ground-based and satellite measurements (e.g., Morton, 1986; Miller and Millis, 1989), but estimating evaporation from a saline lake requires knowledge of changing extent and salinity of the lake and detailed meteorological parameters that were not consistently available for the full extent of our study period during the MODIS era. Therefore we do not provide estimates of trends in evaporation of the GSL over the study period.

3.7 Lake surface-water temperature

In a comprehensive study of the surface-water temperature (SWT) of the Great Salt Lake between 2000 and 2007, Crosman and Horel (2009) used the MODIS Terra MOD11_L2 LST products to measure spatial, diurnal, seasonal, and annual variations in SWT. For the present work, we use the V006 Aqua MODIS daily 1-km resolution daytime and nighttime LST products, MYD21A1D and MYD21A1N, respectively, described above, which represent an advancement over the MOD11 and MYD11 LST products.

First, the approximate minimum areal extent of the lake during the MODIS era was delineated to ensure that dry lake-bed features would not be included in the calculations of SWT. The extent

was delineated using the MODIS MCD43A3 near-infrared white-sky albedo (WSA) product of Schaaf et al. (2002) and Schaaf and Wang (2015), using a MODIS tile acquired on 25 July 2015 during drought conditions when lake water-surface elevation was very low and the areal extent was greatly reduced (see MODIS image in Figure 2 for a 29 July 2015 MODIS image). This minimum extent was used for each day of the LST calculations.

A gap-filling method was used to create daily cloud-free mean-daytime and mean-nighttime SWT maps from 2003 – 2018. Monthly and then annual means for daytime and nighttime were then calculated, excluding pixels affected by thin cirrus, and using cloud flags 0 and 1. The temperature change over the study period (2003-2018) was determined from the values at the beginning and ending of the trend lines. Then the daytime and nighttime trends were averaged to get a mean SWT for the study period.

3.8 Elevation of the water surface and areal extent of the Great Salt Lake

Measurement of the lake surface-water elevation began in 1847, and continued on an irregular basis until the early 1860s when measurements became more regular in most years. On 1 January 1938 (south part) and 15 April 1966 (north part), measurements began on a biweekly or monthly basis, until 1 January 1989 when both become daily. Measurements are now made every 15 minutes by the USGS, and averaged to provide a daily value (USGS, 2019). USGS daily water-surface elevation data from both Saltair Beach State Park in the south arm of the GSL and Little Valley Boat Harbor in the north arm are available from the U.S. Geological Survey (USGS, 2019). These data were used to plot the surface-water elevation of the GSL.

To calculate the areal extent of the GSL from 2000 – 2019 using MODIS 500-m resolution data, the MCD43A3 product was used in the manner described in Section 3.7. Landsat imagery from the Landsat -7 ETM+ on 29 November 2000 and the Landsat-8 OLI on 7 November 2019, was also used because the areal extent of the GSL can be determined more accurately using the finer-resolution Landsat data (30-m resolution) versus MODIS.

4. Results

4.1 Air and surface temperatures in the GSL basin

Air temperatures have increased in the GSL basin since at least 2000, causing more precipitation to fall as rain versus snow and contributing to an increase in evaporation. Based on data from the 26 meteorological stations shown in Figure 4, the change in mean basin air temperature is 0.94°C ($\alpha=0.05$), with a greater increase in the nighttime temperature, or T_{min} (1.40°C ($\alpha=0.01$)) (Table 1).

Table 1. Change in air temperature, 2000 – 2018, in the Great Salt Lake basin, based on the 26 stations shown in Figure 4. Statistical significance is indicated with one asterisk (*) for significance of $\alpha=0.05$, and two asterisks (**) for significance of $\alpha=0.01$.

Change in T_{min} $^{\circ}\text{C}$	Change in T_{max} $^{\circ}\text{C}$	Change in T_{mean} $^{\circ}\text{C}$
1.40**	0.48	0.94*

The mean surface temperature of the GSL basin, or LST, increased by $\sim 2.18^{\circ}\text{C}$ from 2003–2018, with a $\sim 2.04^{\circ}\text{C}$ increase in the daytime LST (MYD21A1D) and a $\sim 2.32^{\circ}\text{C}$ increase in the nighttime LST (MYD21A1N) (Figures 5a and c). Most of the pixels show statistically-significant ($\alpha=0.05$) trends toward increasing surface temperature (Figures 5b and d). More of the nighttime pixels in the basin show statistically significant trends as compared to those in the daytime (Figures 5b and d).

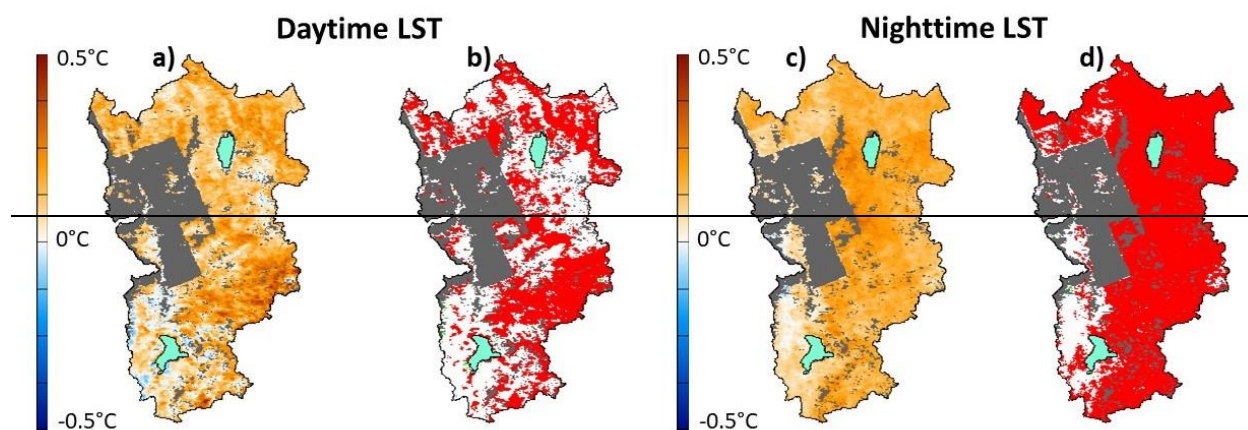


Fig. 5a, b, c & d. Grey represents LST data that were removed due to temporal coverage consistency checks, mainly resulting from corrupted MYD21A1N data; thus to compare daytime and nighttime data, grey areas were removed from all of the maps. a) Mean trends in daytime land-surface temperature (LST) ($^{\circ}\text{C}$) on a per-pixel basis in the Great Salt Lake basin, 2003 – 2018; map developed using the MODIS MYD21A1D (Aqua) standard data product. b) Map showing statistical significance of the trends in Figure 5a for each pixel. Red indicates that the value in that pixel is statistically significant ($\alpha=0.05$) for increasing LST and the very few green pixels in the southwestern part of the basin indicate that the value in that pixel is statistically significant ($\alpha=0.05$) for decreasing LST. c) Mean trends in nighttime LST ($^{\circ}\text{C}$) on a per-pixel basis in the Great Salt Lake basin, 2003 – 2018; map developed using the MODIS MYD21A1N (Aqua) standard data product. d) Map showing statistical significance of the trends in Figure 5c for each pixel. Red indicates that the value in that pixel is statistically significant ($\alpha=0.05$) for increasing LST.

4.2 Snowmelt timing

In the GSL basin, the snowpack was melting on average ~ 9.5 days earlier between WY 2001 – 2018 according to the snowmelt-timing trend map in Figure 6a. Snow is melting earlier at a greater rate at the lower elevations, <2000 m, as expected, since lower elevations tend to be warmer (e.g., Scalzitti et al., 2016). On average, the lower elevations experienced a trend of ~ 10.8 days of earlier snowmelt while the higher elevations, >2000 m, experienced a trend of ~ 8.2 days of earlier snowmelt. Though the vast majority of the statistically-significant trends ($\alpha=0.05$) are associated with earlier snowmelt (red pixels in Figure 6b), there are also 16 pixels showing statistically-significant trends of later snowmelt, all of which occur in the southwestern part of the basin (green pixels in Figure 6b).

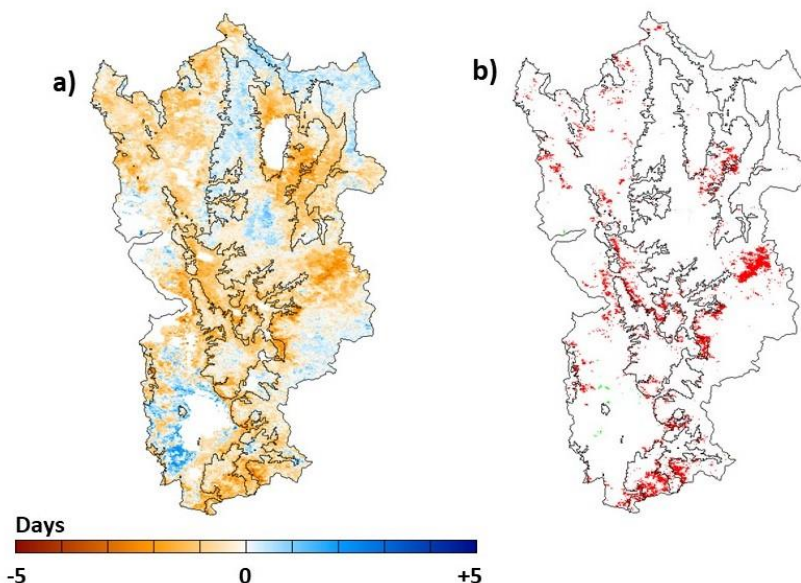


Fig. 6a & b. a) Trends in snowmelt timing in days/yr for the Great Salt Lake basin from WY 2001 – 2018, using a modification of the snowmelt-timing map product of O’Leary et al. (2017). The orange colors indicate earlier snowmelt, while the blue colors represent later snowmelt. b) Pixels for which the trends are statistically significant ($\alpha=0.05$) as shown with red indicate a trend toward earlier snowmelt, and the few (only 16) green pixels in the southwestern part of the basin, indicate a trend toward later snowmelt. The black line delineates the lower (<2000 m) and higher (≥ 2000 m) elevations in both a) and b) as seen in Figure 1.

4.3 Streamflow data

Data from the 12 stream gauges studied reveal a trend toward lower stream discharge over the period of record. The period of record of the gauges varies and is shown in Table 2, along with the trends in discharge in $\text{m}^3/\text{sec}/\text{yr}$; also see Appendix 2. The trends in stream discharge are heavily influenced by stream diversions, so the discharge trends cannot be used to conclude that the streamflow has been declining due to natural events.

Table 2. Trends in stream discharge at USGS stream gauge stations in the Bear, Weber and Jordan rivers in the Great Salt Lake basin from the first full year following the beginning of the station record through 2018.

Station number and name	Record length (yrs)	Size of drainage area (km^2)	Trend in annual discharge ($\text{m}^3/\text{sec}/\text{yr}$) over the period of record
USGS 10011500 BEAR RIVER NEAR UTAH-WYOMING STATE LINE	76	445.48	-0.0002
USGS 10020100 BEAR RIVER ABOVE RESERVOIR, NEAR WOODRUFF, UT	57	1,955.44	-0.0468
USGS 10020300 BEAR RIVER BELOW RESERVOIR, NEAR WOODRUFF, UT	57	2,030.55	-0.0404
USGS 10038000 BEAR RIVER BLW SMITHS FORK, NR COKEVILLE, WY	64	6,337.70	-0.0368
USGS 10039500 BEAR RIVER AT BORDER, WY	81	6,423.17	-0.0013
USGS 10092700 BEAR RIVER AT IDAHO-UTAH STATE LINE	48	12,649.50	-0.5150

USGS 10126000 BEAR RIVER NEAR CORINNE, UT	69	18,205.03	-0.3000
USGS 10128500 WEBER RIVER NEAR OAKLEY, UT	114	419.58	-0.0132
USGS 10129500 WEBER RIVER NEAR WANSHIP, UT	30	867.65	-0.0566
USGS 10136500 WEBER RIVER AT GATEWAY, UT	98	4,213.91	-0.0619
USGS 10141000 WEBER RIVER NEAR PLAIN CITY, UT	70	5,389.77	-0.0983
USGS 10171000 JORDAN RIVER @ 1700 SOUTH @ SALT LAKE CITY, UT	75	8,904.38	-0.0077

4.4 Snowfall, snow depth and snow-water equivalent

During the MODIS era, mean daily snowfall has trended slightly downward at -0.06 mm/yr for a total of -1.1 mm during the study period (not statistically significant), and there has been a decrease in average snow depth, of ~ 34.5 mm ($\alpha=0.01$) in the GSL basin according to meteorological-station data. This decline in snow depth is in general agreement with a previously-reported decline in the snowpack in the Wasatch Mountains at stations below 2400 m (Steenburgh, 2014). There is also a small but statistically-significant ($\alpha=0.01$) trend toward decreasing snow-water equivalent (SWE) in the GSL basin of ~ 0.001 mm/yr, for a total of ~ 0.02 mm, as determined from the SNODAS dataset (NOHRSC, 2004) for WY 2004 - 2018. Earlier snowmelt may account for some of the decrease in snow depth and SWE noted above.

4.5 Evaporation

Evaporation increased in the GSL basin during the MODIS era. For the basin as a whole, there is a mean increase in evaporation of 3.2 mm/yr calculated using the GLEAM dataset from 2000 – 2018 (Figure 7a). Many of the cells, particularly in the northeastern part of the basin show statistically-significant ($\alpha=0.05$) trends toward increasing evaporation (Figure 7b).

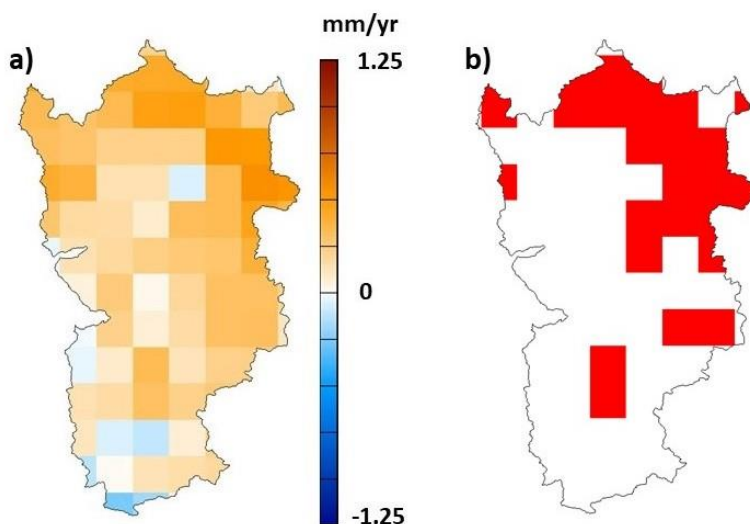


Fig. 7a & b. a) Map showing the trend in rate of evaporation (mm/yr) in the Great Salt Lake basin, 2000 – 2018 from the Global Land surface Evaporation Amsterdam Model (GLEAM) dataset for each 0.25° grid cell in the

basin. b) Map showing statistical significance of the trends shown in a). Red indicates statistical significance ($\alpha=0.05$) for trends of increasing evaporation rate.

4.6 Surface-water temperature of the Great Salt Lake

The mean-monthly SWT of the Great Salt Lake, as measured using the Aqua MODIS LST products (MYD21A1D and MYD21A1N), increased $\sim 0.91^{\circ}\text{C}$ in the daytime and $\sim 0.47^{\circ}\text{C}$ in the nighttime, with an average increase of $\sim 0.69^{\circ}\text{C}$ during the study period (2003 – 2018).

4.7 Elevation and Areal Extent of the Great Salt Lake

Between 1847 and the end of the 2018 WY, the GSL surface-water elevation in the south part of the lake decreased from ~ 1280.1 m to ~ 1277.7 m (Figure 8), however there has been a large amount of variation in the surface-water elevation over the last ~ 170 years, from a high of 1283.7 m (in June 1872, July 1873 and June 1986) (Baskin, 2005), to a low of 1277.5 m (in October of 1963 (USGS, 2019)). From WY 2001 – 2018, daily surface-water elevations from the USGS from both the Saltair Beach State Park (south arm or Gilbert Bay) and from Little Valley Boat Harbor near Saline, Utah (north arm or Gunnison Bay) are plotted in Figure 9. The surface-water elevation at the end of WY 2018 is near the historical low. The difference between the starting and ending elevation on the trend line during this study period is ~ 1.70 m. Each year the lake typically rises ~ 0.61 m in the spring and evaporates ~ 0.61 m of water over the following summer and fall (Jacobsen, 2014) so it is important to compare measurements from the same time of year when calculating changing lake levels because lake-level variations both within and between years can be significant.

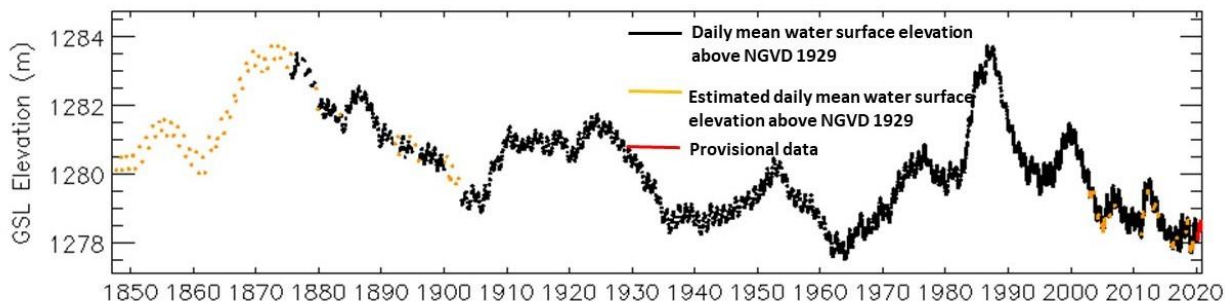


Figure 8. Estimated and measured daily mean lake water-surface elevations of the Great Salt Lake at Saltair Boat Harbor, Utah (USGS, 2019).

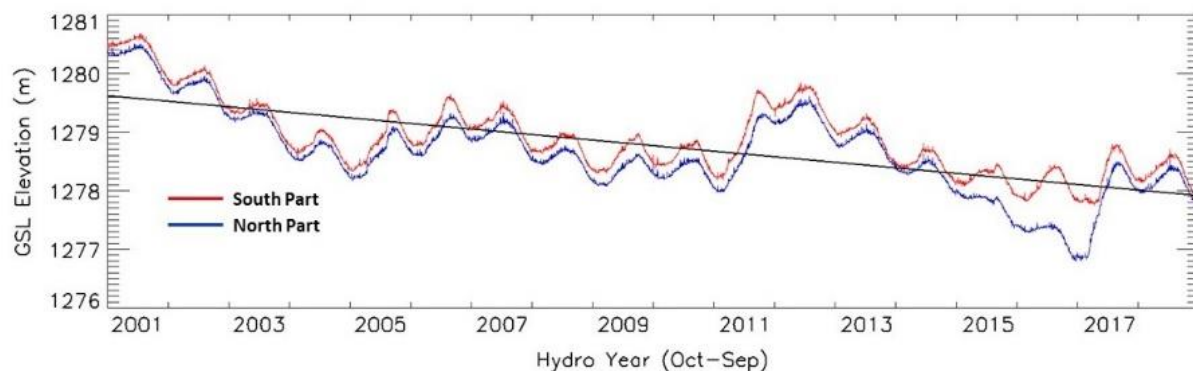


Fig. 9. Daily mean surface-water elevations of the north (Little Valley Boat Harbor near Saline) and south (Saltair Beach State Park) arms of the Great Salt Lake (USGS, 2019). The black line represents the trend, in m/yr, derived from an average of the elevations from the north and south arms of the lake.

The GSL has decreased in area as the surface-water elevation has dropped. The lake shrank from 4022 km² in November of 2000 to 2587 km² in November of 2019, representing a change of ~967 km² as measured from the beginning and end of the trend line, according to measurements using MODIS (500-m resolution) data (Figure 10a & b). According to measurements using the higher-spatial resolution (30-m) Landsat-7 ETM+ and Landsat-8 OLI data, the lake shrank from 3924 km² in November of 2000 to 2685 km² in November of 2019, representing a shrinkage of ~901 km² as measured from the beginning and end of the trend line (Figure 10a & c).

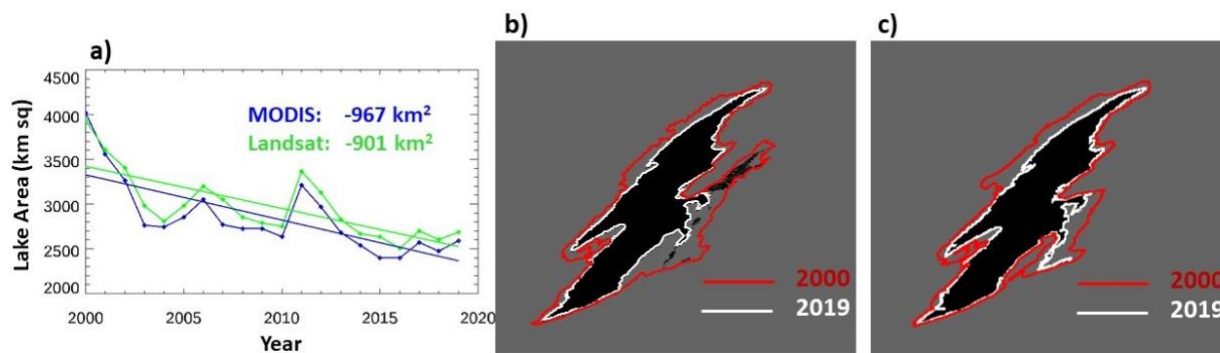


Figure 10a, b & c. a) Graph showing changes in the areal extent of the GSL for each year from 2000 through 2019 using both MODIS and Landsat imagery projected to match the native sinusoidal projection of the MODIS data. b) Change in areal extent of the Great Salt Lake as measured using MODIS imagery. c) Change in areal extent of the Great Salt Lake as measured using Landsat -7 ETM+ and Landsat-8 OLI imagery. b) and c). The outlines for 2019 (white) were obtained from 7 November 2019, and the outlines for 2000 (red) were obtained from 29 November 2000.

5. Discussion and Conclusions

Here, we describe and quantify snow-related, and other environmental factors that contribute to the decline of the GSL using predominantly satellite-based data products. Calculations derived

from independent ground- and satellite-based datasets point to trends of increasing temperatures, less snow and higher evaporation in the GSL basin as a whole. The snowmelt-timing, LST and evaporation trend maps are in general agreement, even in the southwestern part of the GSL basin where the maps show some small areas of trends of patchy daytime cooling, lower evaporation and *later* snowmelt (see Figures 5, 6 and 7).

Air temperatures in much of the western United States have been increasing, and at an accelerated rate in recent decades. Both the air and surface temperatures in the GSL basin show a greater trend toward increasing temperature in the nighttime versus daytime data. Since 2000, mean air temperatures derived from 26 stations in the GSL basin show an increase of $\sim 0.94^{\circ}\text{C}$ ($\alpha=0.05$). The mean LST of the basin measured using the MYD21A1D (daytime) and MYD21A1N (nighttime) MODIS standard data products increased by $\sim 2.18^{\circ}\text{C}$, with most of the pixels in the basin showing statistically significant ($\alpha=0.05$) trends.

Increasing air and surface temperatures in the Great Salt Lake basin have led to less precipitation falling as snow in the springtime, lower snow depth by 34.5 mm ($\alpha=0.01$), lower SWE ~ 0.02 mm ($\alpha=0.01$), and earlier snowmelt by ~ 9.5 days according to snowmelt-timing maps derived from the MOD10A1F snow-cover products. The mean evaporation in the basin increased by ~ 3.2 mm/yr from 2000 – 2018 as determined from the GLEAM dataset. Earlier snowmelt is associated with an increase in evaporation in the basin, and a decrease in streamflow (Milly and Dunne, 2020). USGS stream-gauge records show a general decrease in stream discharge in the GSL basin over the last few decades, though it is not possible to attribute the observed decrease to natural changes because of the many stream diversions that also influence streamflow.

A contributing factor to earlier snowmelt is windblown dust deposition on the snowpack (Skiles et al., 2012, 2015 & 2018; Steenburgh et al., 2012; Reynolds et al., 2014; Maurer and Bowling, 2015). Impurities such as dust in a snowpack increase absorption of solar radiation and decrease albedo (Warren and Wiscombe, 1980). Dust loading in a snowpack can decrease snow-cover duration by several weeks (Painter et al., 2010). Dust that is deposited in the Wasatch Mountains emanates from the Great Basin to the south and west of the GSL as well as from other areas including the dry parts of the GSL lake bed (Steenburgh et al., 2012; Reynolds et al., 2014). A case study by Skiles et al. (2018) shows that dust deposited in the Wasatch Mountains originates primarily from the GSL desert and the dry lake bed to the west of the Wasatch and Uinta ranges. If the dry lake bed of the GSL continues to expand, dust events are likely to increase in frequency perhaps further shortening the duration of the snow-cover season in a positive-feedback loop (Skiles et al., 2018).

Snow cover reflects much of the incident solar radiation back to space thus limiting loss through evaporation (Milly & Dunne, 2020). When snow melts earlier in the springtime, the albedo is lower earlier in the season and evaporative loss increases, resulting in decreased streamflow. Recent works have shown that streamflow decreases with decreasing snowfall even if compensated by an equal amount of rainfall (Bosson et al., 2012; Berghuijs et al., 2014; Milly & Dunne, 2020). Specifically Berghuijs et al. (2014) show that a higher fraction of precipitation falling as snow is associated with higher mean streamflow. Furthermore, a large snowpack can generate runoff more efficiently because rapid spring melt causes soil saturation (Vano et al., 2014). Ultimately, lower streamflow would lead to a lowering of the surface-water elevation of

the GSL since most (66 percent) of the water flowing into the GSL emanates from streamflow. As the lake shrinks, it becomes even more sensitive to changes in streamflow (Maffly, 2015).

The mean surface-water temperature of the Great Salt Lake increased by 0.69°C from 2003-2018 according to measurements using the Aqua MODIS LST data product. Increasing SWT is associated with enhanced evaporation of the lake water leading to a further decline in water level (Miller and Millis, 1989; Hanrahan et al., 2010; Gronewald and Stow, 2014), though total evaporation is reduced by increased salinity and decreased areal extent as the GSL shrinks.

Though the lake levels of the GSL have been lower than they are today (~1277.7 m at the end of WY 2018), with the lowest level (1277.5 m) recorded in 1963, the occasional year or two with a big snowpack cannot compensate for the increasing demand for water in the GSL basin as the population increases in cities and towns along the Wasatch Front.

In short, MODIS and Landsat data show a reduction in the areal extent of the GSL of 967 km² and 901 km², respectively, since 2000. The decline of the Great Salt Lake in Utah has negative consequences for wildlife, recreation, and some lake-related industries. When the lake shrinks, a larger area of the lake bed is exposed which can fuel dust storms. This increases dust pollution and is harmful to human health, and can also enhance snowmelt in the GSL basin.

If air temperatures continue to rise in the GSL basin as predicted (Frankson and Kunkel, 2016), snow cover in the mountains will continue in a trend of earlier melt, and more spring precipitation will fall as rain. Evaporation in the GSL basin and SWT and evaporation in the lake itself will also increase, thus accelerating its decline. However, lessening of drought conditions, and/or changes in water-management practices could decelerate the trend of decline. Time-series data from the Terra, Aqua and Landsat satellites play an important role in observing and documenting environmental factors that contribute to changes in the GSL basin and promote desiccation of the Great Salt Lake, especially when used in conjunction with measured and modeled data. Work is ongoing to study the influence of declining snow in other terminal lake basins in the western United States.

Acknowledgements

We would like to acknowledge support from NASA's Terrestrial Hydrology (grant # 80NSSC18K1674) and Earth Observing Systems programs (grant # NNG17HP01C). Donal O'Leary was supported by the NSF GRFP under grant number DGE-1322106. We thank Dr. Vince Salomonson and Professor John Horel of the University of Utah and Drs. Jim Foster / NASA Emeritus, George Riggs / SSAI, Randy Koster, NASA / Goddard Space Flight Center, and Professor Robert Gurney, University of Reading Emeritus, for helpful discussions regarding this work. In addition, Ryan Rowland / USGS Utah Water Science Center provided invaluable discussions regarding USGS streamflow data. Any opinions, findings, and conclusions or recommendations expressed in this material are those of the authors and do not necessarily reflect the views of NASA or NSF.

References

- Alcott, T.I., Steenburgh, W.J. & Laird, N.F., 2012. Great Salt Lake–effect precipitation: Observed frequency, characteristics, and associated environmental factors. *Weather and forecasting*, 27(4):954-971. <https://doi.org/10.1175/WAF-D-12-00016.1>
- Alcott, T. I. & Steenburgh, W.J., 2013. Orographic Influences on a Great Salt Lake–Effect Snowstorm. *Mon. Wea. Rev.*, 141:2432–2450, <https://doi.org/10.1175/MWR-D-12-00328.1> last accessed: June 16, 2020.
- Arnou, T. & Stephens, D.W., 1990. Hydrologic characteristics of the Great Salt Lake, Utah, 1847-1986 (No. 2332). US Government Printing Office. <https://doi.org/10.3133/wsp2332>
- Audubon, 2020. <https://www.audubon.org/conservation/project/saline-lakes> last accessed 1/12/2020.
- Barnett, T.P., Adam, J.C. and Lettenmaier, D.P., 2005. Potential impacts of a warming climate on water availability in snow-dominated regions. *Nature*, 438(7066), pp.303-309, <https://doi.org/10.1038/nature04141>
- Baskin, R.L., 2005. Calculation of area and volume for the south part of Great Salt Lake, Utah. U.S. Geological Survey Open-File Report 2005–1327. <https://pubs.usgs.gov/of/2005/1327/>
- Bedford, D. & Douglass, A., 2008. Changing properties of snowpack in the Great Salt Lake Basin, Western United States, from a 26-year SNOTEL record. *The Professional Geographer*, 60(3):374-386. <https://doi:10.1080/00330120802013646>
- Berghuijs, W.R., Woods, R.A. and Hrachowitz, M., 2014. A precipitation shift from snow towards rain leads to a decrease in streamflow. *Nature Climate Change*, 4(7):583-586.
- Bosson, E., Sabel, U., Gustafsson, L.G., Sassner, M. and Destouni, G., 2012. Influences of shifts in climate, landscape, and permafrost on terrestrial hydrology. *Journal of Geophysical Research: Atmospheres*, 117(D5), <https://doi.org/10.1029/2011JD016429>
- Carroll, T., Cline, D., Fall, G., Nilsson, A., Li, L. & Rost, A., 2001. NOHRSC Operations and the Simulation of Snow Cover Properties for the Conterminous U.S. *Proceedings of the 69th Annual Meeting of the Western Snow Conference*. pp. 1-14.
- Carson, E.C., 2007. Temporal and seasonal trends in streamflow in the Uinta Mountains, northeastern Utah, and relation to climatic fluctuations. *Arctic, Antarctic, and Alpine Research*. 39(4):521-528. [https://doi:10.1657/1523-0430\(06-072\)\[CARSON\]2.0.CO;2](https://doi:10.1657/1523-0430(06-072)[CARSON]2.0.CO;2)
- Christensen, N. & Lettenmaier, D.P., 2006. A multimodel ensemble approach to assessment of climate change impacts on the hydrology and water resources of the Colorado River Basin. *Hydrology and Earth System Sciences Discussions*. 3(6):3727-3770. www.hydrol-earth-syst-sci-discuss.net/3/3727/2006/

- Crosman, E.T. & Horel, J.D., 2009. MODIS-derived surface temperature of the Great Salt Lake, *Remote Sensing of Environment*. 113(1):73-81. <https://doi.org/10.1016/j.rse.2008.08.013>
- DeRose, R.J., Wang, S.Y., Buckley, B.M. & Bekker, M.F., 2014. Tree-ring reconstruction of the level of Great Salt Lake, USA. *The Holocene*, 24(7):805-813.
- Derouin, S., 2017. Utah's Great Salt Lake has lost half of its water, thanks to thirsty humans. *Science*. <https://www.sciencemag.org/news/2017/11/utah-s-great-salt-lake-has-lost-half-its-water-thanks-thirsty-humans>
- Frankson, R., & Kunkel, K.E., 2016. NOAA NCEI, State Summaries 149-UT, 4pp. <https://statesummaries.ncics.org/ut> - last accessed 1/18/2020.
- Friends of the Great Salt Lake, 2020. <https://www.fogsl.org/research-resources/about-the-lake> – last accessed 8/6/2020.
- Gillies, R.R., Wang, S.Y. & Booth, M.R., 2012. Observational and synoptic analyses of the winter precipitation regime change over Utah. *Journal of Climate*, 25(13):4679-4698. <https://doi.org/10.1175/JCLI-D-11-00084.1>
- GLEAM, 2019. Global Land surface Evaporation Amsterdam Model, European Space Agency, Ghent University & Vrije Universiteit Amsterdam, Read-me file. <https://www.gleam.eu/> last accessed 7/20/2020
- Great Salt Lake Information System, 2020. <http://www.greatsaltlakeinfo.org/Background/Description> last accessed 1/18/2020
- Gronewold, A. D. & Stow, C.A., 2014. Water loss from the Great Lakes. *Science*. 343(6175):1084-1085. <https://doi:10.1126/science.1249978>
- Hall, D. K., Riggs, G.A., Foster, J.L. & Kumar, S.V., 2010. Development and evaluation of a cloud-gap-filled MODIS daily snow-cover product. *Remote Sensing of Environment*, 114(3):496-503. <https://doi.org/10.1016/j.rse.2009.10.007>
- Hall, D.K., Riggs, G.A., DiGirolamo, N.E. & Román, M.O., 2019. Evaluation of MODIS and VIIRS cloud-gap-filled snow-cover products for production of an Earth science data record. *Hydrology and Earth System Science*. <https://doi.org/10.5194/hess-23-5227-2019>
- Hanrahan, J. L., Kravtsov, S. & Roebber, P.J., 2010. Connecting past and present climate variability to the water levels of Lakes Michigan and Huron. *Geophysical Research Letters*. 37(1). <https://doi.org/10.1029/2009GL041707>
- Hulley, G., 2017. MYD21A1D MODIS/Aqua Land Surface Temperature/3-Band Emissivity Daily L3 Global 1km SIN Grid Day V006 [Data set]. NASA EOSDIS Land Processes DAAC. <https://lpdaac.usgs.gov/products/myd21a1dv006/> last accessed 4/16/2020]

Hulley, G. & Hook, S., 2017. MOD21A1D MODIS/Terra Land Surface Temperature/3-Band Emissivity Daily L3 Global 1km SIN Grid Day V006 [Data set]. NASA EOSDIS Land Processes DAAC. <https://lpdaac.usgs.gov/products/mod21a1dv006/> last accessed 5/5/2020

Jacobsen, 2014. Water levels in Great Salt Lake approach record low. Deseret News, Salt Lake City, UT. <https://www.deseret.com/2014/8/22/20547176/water-levels-in-great-salt-lake-approach-record-low#visitors-walk-around-in-the-water-wednesday-aug-20-2014-at-the-great-salt-lake> last accessed 6/12/2020

Lall, U. and Mann, M., 1995. The Great Salt Lake: A barometer of low-frequency climatic variability. *Water Resources Research*, 31(10):2503-2515.

Maffly, B., 2015. Great Salt Lake at near-record low level. The Salt Lake Tribune, February 1, 2015.

Mann, M.E., Lall, U. & Saltzman, B., 1995. Decadal-to-centennial-scale climate variability: Insights into the rise and fall of the Great Salt Lake. *Geophysical Research Letters*, 22(8):937-940. <https://doi.org/10.1029/95GL00704>

Manning, A. H., 2002. Using noble gas tracers to investigate mountain-block recharge to an intermountain basin. PhD dissertation, Department of Geology and Geophysics, University of Utah, 2002.

Martens, B., Gonzalez Miralles, D., Lievens, H., Van Der Schalie, R., De Jeu, R.A., Fernández-Prieto, D., Beck, H.E., Dorigo, W. & Verhoest, N., 2017. GLEAM v3: Satellite-based land evaporation and root-zone soil moisture. *Geoscientific Model Development*, 10(5):1903-1925. <https://doi.org/10.5194/gmd-10-1903-2017>

Maurer, G. E., & Bowling, D.R., 2015. Dust effects on snowpack melt and related ecosystem processes are secondary to those of forest canopy structure and interannual snowpack variability. *Ecohydrology*. 8(6):1005-1023. <https://doi.org/10.1002/eco.1558>

McCabe, G. J. & Wolock, D.M., 2007. Warming may create substantial water supply shortages in the Colorado River basin, *Geophysical Research Letters*. 34, L22708, <https://doi.org/10.1029/2007GL031764>

McKenzie, D. & Littell, J.S., 2017. Climate change and the eco-hydrology of fire: Will area burned increase in a warming western USA? *Ecological Applications*. 27(1):26-36. <https://doi.org/10.1002/eap.1420>

Miller, W. & Millis, E., 1989. Estimating evaporation from Utah's Great Salt Lake using thermal infrared satellite imagery. *Water Resources Bulletin*. 25(3):541-550. <https://doi.org/10.1111/j.1752-1688.1989.tb03090.x>

- Miralles, D.G., Holmes, T.R.H., De Jeu, R.A.M., Meesters, A.G.C.A. & Dolman, A.J., 2011. Global land-surface evaporation estimated from satellite-based observations, *Hydrology and Earth System Science*, 15:453-469. <https://doi:10.5194/hess-15-453-2011>
- Milly, P.C. & Dunne, K.A., 2020. Colorado River flow dwindles as warming-driven loss of reflective snow energizes evaporation. *Science*, 367(6483):1252-1255. <https://doi:10.1126/science.aay9187>
- Mohammed, I.N. & Tarboton, D.G., 2012. An examination of the sensitivity of the Great Salt Lake to changes in inputs. *Water Resources Research*, 48, W1151. <https://doi.org/10.1029/2012WR011908>
- Morton, F.I., 1986. Practical estimates of lake evaporation. *Journal of Climate and Applied Meteorology*, 25:371-387. [https://doi.org/10.1175/1520-0450\(1986\)025<0371:PEOPLE>2.0.CO;2](https://doi.org/10.1175/1520-0450(1986)025<0371:PEOPLE>2.0.CO;2)
- Mote, P.W., Li, S., Lettenmaier, D.P., Xiao, M. and Engel, R., 2018. Dramatic declines in snowpack in the western US. *Npj Climate and Atmospheric Science*, 1(1):1-6.
- NASA Worldview, 2020. <https://earthdata.nasa.gov/worldview> last accessed 5/4/2020]
- NOAA, 2020. <https://gis.ncdc.noaa.gov/maps/ncei/summaries/daily> last accessed 8/4/2020.
- NOHRSC, 2004. National Operational Hydrologic Remote Sensing Center, *Snow Data Assimilation System (SNODAS) Data Products at NSIDC, Version 1*. Boulder, Colorado USA. NSIDC: National Snow and Ice Data Center. <https://doi.org/10.7265/N5TB14TC> last accessed 1/17/2020.
- O'Leary III, D., Hall, D.K., Medler, M., Matthews, R. & Flower, A., 2017. Snowmelt timing maps derived from MODIS for North America, 2001-2015. ORNL DAAC. <https://doi.org/10.3334/ORNLDAAC/1504>
- O'Leary, D., Hall, D., Medler, M. & Flower, A., 2018. Quantifying the early snowmelt event of 2015 in the Cascade Mountains, USA by developing and validating MODIS-based snowmelt timing maps. *Frontiers of Earth Science*, 12(4):693-710. <https://doi.org/10.1007/s11707-018-0719-7>
- O'Leary, D., Hall, N.E. DiGirolamo & G.A. Riggs, 2020. Regional trends in snowmelt timing for the western United States throughout the MODIS era, in press.
- Painter, T.H., Deems, J.S., Belnap, J., Hamlet, A.F., Landry, C.C. & Udall, B., 2010. Response of Colorado River runoff to dust radiative forcing in snow. *Proceedings of the National Academy of Sciences*, 107(40):17125-17130. <https://doi.org/10.1073/pnas.0913139107>
- Penrod, E., 2019. Scientists say the Great Salt Lake is disappearing, but could Utah residents save it? The Salt Lake Tribune.

Priestly, C.H.B. & Taylor, R.J., 1972. On the assessment of surface heat flux and evaporation using large-scale parameters. *Monthly Weather Review*. 100:81-92.

Reynolds, R.L., Goldstein, H.L., Moskowitz, B.M., Bryant, A.C., Skiles, S.M., Kokaly, R.F., Flagg, C.B., Yauk, K., Berquó, T., Breit, G. & Ketterer, M., 2014. Composition of dust deposited to snow cover in the Wasatch Range (Utah, USA): Controls on radiative properties of snow cover and comparison to some dust-source sediments. *Aeolian Research*, 15:73-90.
<https://doi.org/10.1016/j.aeolia.2013.08.001>

Riggs, G. A., Hall, D. K., & Román, M.O., 2017. Overview of NASA's MODIS and Visible Infrared Imaging Radiometer Suite (VIIRS) snow-cover. *Earth Syst. Sci. Data*. 9:1–13,
<https://doi.org/10.5194/essd-9-765-2017>

Riggs, G. A., Hall, D. K., & Román, M.O., 2018. MODIS snow products user guide for Collection 6.1 (C6.1). Available at: <https://modis-snow-ice.gsfc.nasa.gov/?c=userguides> last accessed 3/17/2019.

Schaaf, C.B., Gao, F., Strahler, A.H., Lucht, W., Li, X., Tsang, T., Strugnell, N.C., Zhang, X., Jin, Y., Muller, J.P. & Lewis, P., 2002. First operational BRDF, albedo nadir reflectance products from MODIS. *Remote sensing of Environment*, 83(1-2):135-148.
[https://doi.org/10.1016/S0034-4257\(02\)00091-3](https://doi.org/10.1016/S0034-4257(02)00091-3)

Schaaf, C. & Wang, Z., 2015. MCD43A3 MODIS/Terra+Aqua BRDF/Albedo Daily L3 Global - 500m V006. NASA EOSDIS Land Processes DAAC. Accessed 2020-05-05 from
<https://doi.org/10.5067/MODIS/MCD43A3.006>

Scalzitti, J., C. Strong & A. Kochanski, A., 2016. Climate change impact on the roles of temperature and precipitation in western U.S. snowpack variability, *Geophys. Res. Lett.*, 43:5361–5369, <https://doi.org/10.1002/2016GL068798>.

Skiles, S.M., Painter, T.H., Deems, J.S., Bryant, A.C. & Landry, C.C., 2012. Dust radiative forcing in snow of the Upper Colorado River Basin: 2. Interannual variability in radiative forcing and snowmelt rates. *Water Resources Research*, 48(7). <https://doi.org/10.1029/2012WR011986>

Skiles, S.M., Painter, T.H., Belnap, J., Holland, L., Reynolds, R.L., Goldstein, H.L. & Lin, J., 2015. Regional variability in dust-on-snow processes and impacts in the Upper Colorado River Basin. *Hydrological Processes*, 29(26):5397-5413. <https://doi.org/10.1002/hyp.10569>

Skiles, S.M., Mallia, D.V., Hallar, A.G., Lin, J.C., Lambert, A., Petersen, R. & Clark, S., 2018. Implications of a shrinking Great Salt Lake for dust on snow deposition in the Wasatch Mountains, UT, as informed by a source to sink case study from the 13–14 April 2017 dust event. *Environmental Research Letters*, 13(12), p.124031. <https://doi.org/10.1088/1748-9326/aaefd8>

SNODAS, 2020. Available through NSIDC <https://nsidc.org/data/g02158> - last accessed 7/14/2020

SNOTEL, 2020. USDA, NRCS and National Water and Climate Center, <https://www.wcc.nrcs.usda.gov/snow/> - last accessed 8/6/2020.

Steenburgh, J., 2014. Secrets of the Greatest Snow on Earth. University Press of Colorado.

Steenburgh, W.J., & Alcott, T.I., 2008. Secrets of the “Greatest Snow on Earth.” *Bulletin of the American Meteorological Society*. 89(9):1285-1294. <https://doi.org/10.1175/2008BAMS2576.1>

Steenburgh, W.J., Halvorson, S.F. & Onton, D.J., 2000. Climatology of lake-effect snowstorms of the Great Salt Lake. *Monthly Weather Review*, 128(3), pp.709-727. [https://doi.org/10.1175/1520-0493\(2000\)128<0709:COLESO>2.0.CO;2](https://doi.org/10.1175/1520-0493(2000)128<0709:COLESO>2.0.CO;2)

Steenburgh, W.J., Massey, J.D. & Painter, T.H., 2012. Episodic dust events of Utah’s Wasatch Front and adjoining region. *Journal of Applied Meteorology and Climatology*, 51(9):1654-1669. <https://doi.org/10.1175/JAMC-D-12-07.1>

Udall, B., & Overpeck, J., 2017. The twenty-first century Colorado River hot drought and implications for the future. *Water Resources Research*. 53(3):2404-2418. <https://doi.org/10.1002/2016WR019638>

USGS, 2007. Great Salt Lake, Utah. Water-Resources Investigations Report 1999–4189, April 2007.

USGS, 2019. National Water Information System <https://waterdata.usgs.gov/ut/nwis/current?type=lake> last accessed 7/15/2020.

USGS, 2020. National Water Information System: Web Interface <https://waterdata.usgs.gov/nwis/rt> last accessed 7/17/2020.

USGS GTOPO30 DEM, 2019. https://www.usgs.gov/centers/eros/science/usgs-eros-archive-digital-elevation-global-30-arc-second-elevation-gtopo30?qt-science_center_objects=0#qt-science_center_objects last accessed 12/12/2019

USGS National Map, 2019. https://nationalmap.gov/small_scale/mld/1strmsl.html last accessed 12/12/2019

Utah Geological Survey, 2020: <https://geology.utah.gov/popular/general-geology/great-salt-lake/commonly-asked-questions-about-utahs-great-salt-lake-lake-bonneville/#toggle-id-7> last accessed 7/15/2020

Utah’s Watershed Restoration Initiative, 2019. Weber River Morgan Area Restoration. <https://wri.utah.gov/wri/reports/ProjectSummaryReport.html?id=4629> last accessed 7/21/2020

- Utah Water Science Center, 2020. https://www.usgs.gov/centers/ut-water/science/bear-lake-water-quality?qt-science_center_objects=0#qt-science_center_objects last accessed 8/6/2020.
- Vano, J.A., Udall, B., Cayan, D.R., et al., 2014: Understanding Uncertainties in Future Colorado River Streamflow. *Bull. Amer. Meteor. Soc.*, 95:59–78. <https://doi.org/10.1175/BAMS-D-12-00228.1>
- Wang, S.Y., Gillies, R.R., Jin, J. & Hipps, L.E., 2010. Coherence between the Great Salt Lake level and the Pacific quasi-decadal oscillation. *Journal of Climate*, 23(8):2161-2177.
- Wang, S.Y., Gillies, R.R. and Reichler, T., 2012. Multidecadal drought cycles in the Great Basin recorded by the Great Salt Lake: Modulation from a transition-phase teleconnection. *Journal of Climate*, 25(5):1711-1721. <https://doi.org/10.1175/2011JCLI4225.1>
- Wang, J., Song, C., Reager, J.T., Yao, F., Famiglietti, J.S., Sheng, Y., MacDonald, G.M., Brun, F., Schmied, H.M., Marston, R.A. & Wada, Y., 2018. Recent global decline in endorheic basin water storages. *Nature Geoscience*, 11:926-932. <https://doi.org/10.1038/s41561-018-0265-7>
- Warren, S.G. and Wiscombe, W.J., 1980. A model for the spectral albedo of snow. II: Snow containing atmospheric aerosols. *Journal of the Atmospheric Sciences*, 37(12):2734-2745. [https://doi.org/10.1175/1520-0469\(1980\)037<2734:AMFTSA>2.0.CO;2](https://doi.org/10.1175/1520-0469(1980)037<2734:AMFTSA>2.0.CO;2)
- White, J.S., S.E. Null & D. Tarboton, 2014. More than meets the eye: Managing salinity in the Great Salt Lake, Utah, *LakeLine Magazine*, 34(3):25-29. <https://www.nalms.org/nalms-memberships/>
- Williams, A.P., Cook, E.R., Smerdon, J.E., Cook, B.I., Abatzoglou, J.T., Bolles, K., Baek, S.H., Badger, A.M. & Livneh, B., 2020. Large contribution from anthropogenic warming to an emerging North American megadrought. *Science*, 368(6488):314-318. <https://doi:10.1126/science.aaz9600>
- Wurtsbaugh, W.A., Miller, C., Null, S.E., Wilcock, P., Hahnenberger & M., Howe, F., 2016. Impacts of water development on Great Salt Lake and the Wasatch Front, Utah State University Watershed Sciences Faculty Publications, White Paper, 24 February 2016, available at: https://works.bepress.com/wayne_wurtsbaugh/171/
- Wurtsbaugh, W.A., Miller, C., Null, S.E., DeRose, R.J., Wilcock, P., Hahnenberger, M., Howe, F. & Moore, J., 2017. Decline of the world's saline lakes. *Nature Geoscience*, 10(11):816-821. <https://doi.org/10.1038/ngeo3052>
- Yeager, K.N., Steenburgh, W.J. and Alcott, T.I., 2013. Contributions of lake-effect periods to the cool-season hydroclimate of the Great Salt Lake basin. *Journal of Applied Meteorology and Climatology*, 52(2):341-362. <https://doi.org/10.1175/JAMC-D-12-077.1>

Appendix 1. National Weather Service and SNOTEL meteorological stations in the effective area of the Great Salt Lake basin as defined in this work. USDA Natural Resources Conservation Service and National Water and Climate Center SNOTEL stations [<https://www.wcc.nrcs.usda.gov/snow/>] are indicated by an asterisk (*).

Name and State	Latitude (°)	Longitude (°)	Elevation (m)
Alpine, UT	40.464	-111.771	1555
Alta, UT	40.591	-111.637	2655
Beaver Divide, UT*	40.617	-111.100	2524
Ben Lomond Peak, UT*	41.383	-111.950	2344
Bern HCN, ID	42.335	-111.385	1818
Bountiful Bench, UT	40.854	-111.890	1384
Brigham City Waste Plt., UT	40.891	-111.850	1289
Bug Lake, UT	41.683	-111.417	2423
City Creek Wtp., UT	40.816	-111.835	1625
Cutler Dam, UT	41.833	-112.055	1308
Dry Bread Pond, UT	41.417	-111.533	2545
Franklin Basin, ID	42.049	-111.599	2451
Kamas, UT	40.643	-111.282	1974
Laketown HCN, UT	41.826	-111.321	1823
Lifton Pumping Station HCN, ID	42.123	-111.313	1809
Logan 5 SW Exp. Frm., UT	41.667	-111.890	1369
Logan Radio KVNU, UT	41.735	-111.856	1364
Logan Utah St. Univ. HCN, UT	41.746	-111.803	1460
Nephi HCN, UT	39.713	-111.832	1562
Parrish Creek, UT*	40.933	-111.817	2359
Provo BYU, UT	40.244	-111.650	1393
Richmond, UT	41.906	-111.810	1427
Salt Lake City Intl., UT	40.778	-111.969	1288
Santaquin Chlorinator, UT	39.958	-111.779	1573
Trial Lake, UT*	40.680	-110.950	3046
Woodruff HCN, UT	41.525	-111.149	1925

Appendix 2. Name, number, coordinates, elevation and start year of stream gauges from the Bear River, Weber River and Jordan River in the Great Salt Lake basin, that were used in this manuscript. Data were obtained from the U.S. Geological Survey.

BEAR RIVER		NGVD 29		
(Gages are listed from highest to lowest elevation)		Coordinates	Elev (m)	Start (yr)
USGS 10011500	BEAR RIVER NEAR UTAH-WYOMING STATE LINE	40°57'55", 110°51'10"	2428.35	1943
USGS 10020100	BEAR RIVER ABOVE RESERVOIR*, NEAR WOODRUFF, UT	41°26'04", 111°01'01"	1967.99	1962
USGS 10020300	BEAR RIVER BELOW RESERVOIR*, NEAR WOODRUFF, UT	41°30'20", 111°00'50"	1951.22	1962
USGS 10038000	BEAR RIVER BLW SMITHS FORK, NR COKEVILLE, WY	42°07'36", 110°58'21"	1871.95	1955
USGS 10039500	BEAR RIVER AT BORDER, WY	42°12'40", 111°03'11"	1845.01	1938
USGS 10092700	BEAR RIVER AT IDAHO-UTAH STATE LINE	42°00'47", 111°55'14"	1347.56	1971
USGS 10126000	BEAR RIVER NEAR CORINNE, UT	41°34'35", 112°06'00"	1281.89	1950
*Woodruff Narrows Reservoir				
Cutler Reservoir				
WEBER RIVER		Coordinates	Elev (m)	Start (yr)
USGS 10128500	WEBER RIVER NEAR OAKLEY, UT	40°44'14", 111°14'50"	2024.39	1905
USGS 10129500	WEBER RIVER NEAR WANSHIP, UT	40°47'34", 111°24'15"	1798.78	1989
USGS 10136500	WEBER RIVER AT GATEWAY, UT	41°08'13", 111°49'54"	1463.41	1921
USGS 10141000	WEBER RIVER NEAR PLAIN CITY, UT	41°16'42", 112°05'28"	1282.65	1949
JORDAN RIVER		Coordinates	Elev (m)	Start (yr)
USGS 10171000	JORDAN RIVER @ 1700 SOUTH @ SALT LAKE CITY, UT	40°44'01", 111°55'21"	1286.61	1944